

# Raman spectroscopic study of dilute HOD in liquid H<sub>2</sub>O in the temperature range — 31.5 to 160 °C

D. E. Hare and C. M. Sorensen

*Department of Physics, Kansas State University, Manhattan, Kansas 66506*

(Received 6 June 1990; accepted 8 August 1990)

We present Raman data for the OD stretch mode of 10 mol % HOD in H<sub>2</sub>O for the liquid phase from — 31.5 to 160 °C. We find that an exact isosbestic does not hold, but rather the crossing of isotherms slowly but uniformly changes with temperature. We present an analysis based on Boltzmann statistics which gives evidence for a distribution of deuterium hydrogen bond strengths with minimum energy near the frequency (2440 cm<sup>-1</sup>) also found in the solid ice and amorphous solid phases. This analysis also gives evidence for a band of frequencies above 2630 cm<sup>-1</sup> due to OD oscillators all at essentially the same high energy relative to the strongest hydrogen bonds, and we interpret this band as due to broken hydrogen bonds. This allows us to calculate hydrogen bond probabilities, and we find this probability increases with decreasing temperature and approaches a value equal to the four bonded percolation threshold near the singular temperature  $T_s \simeq -45$  °C for the anomalies of supercooled water. Peak frequency and full width at half-maximum of the OD stretch band are found to drop precipitously to the amorphous solid values as  $T \rightarrow T_s$ , implying the ultimate state of supercooled water is similar to the amorphous solid.

## I. INTRODUCTION

Dilute deuterium doping of liquid water has long been a useful tool for studying water's intramolecular stretch spectrum. When a small amount of D<sub>2</sub>O is added to H<sub>2</sub>O, water's hydrogen bonded structure remains virtually unchanged yet the Raman spectrum of the OD oscillators becomes greatly simplified. The more massive OD oscillators cannot strongly couple to the dominant component OH oscillators, and if dilute, their scarcity isolates them from each other. Thus isolated, the Raman spectrum of the OD stretch of this system principally reflects the local OD oscillator environment. This greatly simplifies its relationship to the distribution functions describing the properties of individual hydrogen bonds. In this paper we use this idea to study the hydrogen bonding properties of water over a broad temperature range including the deeply supercooled regime.

Raman studies on this system go back at least to 1965 when Wall and Hornig obtained a single broad OD band displaying only slight asymmetry.<sup>1</sup> Lack of evidence for two or more distinct peaks caused them to favor an interpretation involving a continuum distribution of hydrogen bond properties. Walrafen's subsequent work of higher resolution displayed this asymmetry more clearly as having the appearance of a definite high frequency shoulder.<sup>2</sup> In addition, he obtained a frequency of temperature independent intensity, that is, an isosbestic crossing of his isotherms. This type of behavior is indicative of two-state behavior. Both Walrafen<sup>2</sup> and Scherer *et al.*<sup>3</sup> have used two-band decompositions of this region with good results. More recently, Bansil *et al.* performed a two-state separation of the uncoupled OD stretch in the supercooled liquid.<sup>4</sup> To obtain the nonhydrogen bonded component width they assumed symmetry of the dominant low frequency peak about its maximum to remove

the high frequency shoulder. This shoulder represented the nonhydrogen bonded OD oscillator component. Their analysis led to a rather large value for deuterium bond probability (0.90 at 0 °C). This value is well above the four bonded percolation threshold predicted to occur at  $p_{HB} = 0.795$ ,<sup>5</sup> and therefore not consistent with percolation theories of the anomalous properties of supercooled liquid water near — 45 °C.

The problem of describing the source of the anomalies in supercooled water has occupied considerable interest since their original characterization by Speedy and Angell in 1976.<sup>6</sup> It is generally conceded that it is water's self-association through hydrogen bonding and subsequent unique volumetric properties due to its tetrahedral configurations that lead to these anomalies. Questions remain regarding the ultimate state of water if it were to achieve the extrapolated singular temperature  $T_s \simeq -45$  °C, and how apparently random association through hydrogen bonds can lead to singular behavior which is often indicative of cooperative phenomena. Raman scattering, particularly in the OH stretch regime, is sensitive to hydrogen bonding and has been useful in elucidating this problem. Recently, Green, Lacey, and Sceats<sup>7</sup> and ourselves<sup>8</sup> have given evidence that a large collective mode develops in supercooled pure H<sub>2</sub>O and this mode is approaching that found in amorphous solid water as the liquid approaches  $T_s$ . Our work qualitatively supported the percolation theories and suggested that the infinite percolation cluster had the structure of the amorphous solid. The precise nature of single OH oscillators, however, is difficult to infer from data on pure H<sub>2</sub>O due to extensive intra- and intermolecular coupling, especially in the supercooled regime where hydrogen bonding is greatest. Thus, it is valuable to study uncoupled OD in dilute HOD solutions in or-

der to gain information on individual hydrogen bonds in the deeply supercooled regime.

In this paper, we present the Raman  $I_{VV}$  polarization spectra of the OD stretch of 10 mol % of HOD in liquid H<sub>2</sub>O covering the temperature range  $-31.5$  to  $+160$  °C. These spectra are quantitative in the sense that intensity between any two different isotherms may be quantitatively compared. This allows us to carefully examine the isosbestic behavior over 191 °C of temperature range thus investigating certain limitations of the two-state hypothesis.

We also present an analysis based on Boltzmann statistics that show a distribution of hydrogen bond strengths and a separate class consistent with the concept of broken hydrogen bonds. We use this to calculate the hydrogen bond probability and show its temperature dependence is consistent with percolation theories. We also show the peak frequencies and full width at half-maximum of the OD stretch band rapidly approach the values of the amorphous solid in the region of  $T_g$ . Our conclusions will support the concept that supercooled water is approaching a percolation threshold with structure similar to that of the amorphous solid.

## II. EXPERIMENTAL METHOD

Much of our experimental technique and apparatus was similar to our earlier study of pure H<sub>2</sub>O.<sup>8</sup>

### A. Description of samples

Two sets of samples were made. One set contained 10 mol % HOD in H<sub>2</sub>O, the other set was additionally doped with 1 mol % CH<sub>3</sub>OH. The undoped (with methanol) samples were prepared by Mossop's method.<sup>9</sup> One liter of solution was placed in a simple distiller which exited to the atmosphere through a standard 5 mm Pyrex tube. About 3/4 of the sample was boiled off to purge the distiller of ice forming nuclei and cleanse the tube with hot steam. The tube was then pulled into a large (about 500  $\mu$ m i.d.) capillary with an oxy methane flame while steam continued to pass through it. It was flamed sealed at the bottom and allowed to fill with the pure condensate, then sealed at the top, leaving a small amount of vapor space to allow for sample expansion. The process was repeated until the tube was used up. The results were large capillaries filled only with pure samples. Their fresh interior surface had never been exposed to the nuclei polluted room air. Roughly 20% of the samples prepared in this manner could be supercooled to  $-33$  °C, the apparent homogeneous nucleation temperature. This method was not applied to the doped solutions to avoid possible pyrolysis of the methanol content. Therefore, an alternate method was devised. Standard 5 mm tube was washed with soap and boiled in distilled water. It was then pulled into large capillaries, filled with the doped solution, and carefully flame sealed. The sealed capillaries were heat treated at  $+120$  °C for 20 h followed by treatment at  $+160$  °C for 2 h. This method produced two samples out of 11 that nucleated below  $-33$  °C. It appeared that the hot sample water could dissolve potential heterogeneous nuclei, permitting deep supercooling. This second method appears to be an alternative to Mossop's method for achieving homogeneous nucleation.

Both methods produced large ( $> 300$   $\mu$ m i.d.) samples of good optical quality that could be supercooled to their homogenous nucleation limit. The resultant Raman spectra were of high quality and without significant surface effects. The samples prepared by the Mossop method are under the vapor pressure of water. Doped samples also contain the air left in the vapor space during sealing. Maximum pressure (at 160 °C) on the samples is not expected to exceed 6000 mm of Hg. This pressure has little effect.

### B. Raman setup

Excitation was accomplished by a plane polarized argon ion laser beam of 100 mW power with  $\lambda = 4880$  Å. The scattered light was collected at 90° to both the incident direction and plane of vibration, collimated by an  $f/1.7$  camera lens, passed through a polarized analyzer (extinction ratio  $< 10^{-3}$ ) and directed and condensed into the spectrometer. The spectrometer was a SPEX 1404 0.85 m double spectrometer equipped with a Hamamatsu R943-02 Raman photomultiplier tube, refrigerated to suppress thermal noise. The output was first discriminated and shaped by a PAD, then sent to a computer where it could be stored and analyzed.

### C. Temperature control

Below  $+100$  °C the sample was mounted in a copper cell having an outer jacket with temperature equal to that at the scattering volume to minimize thermal gradients. Thermal contact of the scattering volume was facilitated by dry nitrogen, which oozed out over the sample after coming to thermal equilibrium with the cell's interior. Temperature was maintained by methanol (or water above  $+30$  °C) pumped from a Neslab Ex 300 DD bath fitted with two mechanical refrigeration probes. Temperature was measured by a thermistor calibrated against NBS traceable thermometers. Its uncertainty was  $\pm 0.5$  °C in this cell.

Above  $+100$  °C the sample was mounted in an aluminum cell with silicone gasket glue. Cell temperature was maintained by an RTD controlled resistance heating element. Here, dry nitrogen was also used to facilitate sample to cell contact. Temperature was measured by a Hg in glass thermometer placed in a deep hole in the top of the cell. A small correction was necessary to account for a slight gradient between the thermometer and sample position. Temperature uncertainty was  $\pm 1$  °C in this cell.

### D. Spectral corrections and characteristics

The spectrometer and associated optics were calibrated with a standard lamp, and this correction was applied to all the spectra.

There was significant background intensity due partly to fluorescence from the capillary's Pyrex walls and partly to combination bands from the sample's H<sub>2</sub>O component. For the doped spectra used to deduce integrated OD intensity vs temperature, a linear background removal was adequate. For the remaining spectra, the background was formed from spectra of a capillary containing pure H<sub>2</sub>O normalized to fit the wings on each side of the OD band. Once the background

was subtracted, these same spectra were each renormalized by an appropriate constant determined from the calibration described below to make  $I$  vs  $T$  quantitative.

The Placzek (i.e., "Bose Einstein") correction was not performed on any of the spectra. Its temperature dependence is insignificant in the OD stretch region, even at 160 °C. Its frequency dependence is important in the quantitative calculation of hydrogen bond probability, where it was accounted for in the analysis.

The spectrometer was operated with a 15 cm<sup>-1</sup> band-pass and channel width in the digitized spectra was 10 cm<sup>-1</sup>. The methanol doped spectra were used for their integrated intensities. They are the average of two 100 s scans. The remaining spectra are the average of 20 such scans and have excellent signal to noise ratio. All are of the  $I_{VV}$  polarization.

### III. DATA ANALYSIS

#### A. Calibration of spectra

The Raman spectroscopist has traditionally had to go to considerable trouble to obtain spectra which could be quantitatively compared over a range of temperatures. To obtain such spectra requires stability and control of the laser excitation, correction for density and index of refraction variation with temperature, and careful cell alignment and stability. This latter difficulty limited past work of this type to optical cuvettes.<sup>10,11</sup>

We have been able to avoid these difficulties and achieve precise calibration in capillary samples by doping with a small amount of methanol. Methanol has an intense CH stretch band at 2837 cm<sup>-1</sup> which is very insensitive to temperature and hydrogen bond environment. We used a 1 mol % solution of methanol in water which was found to be a good compromise between an adequate calibration intensity and a negligible effect on the liquid water's hydrogen bonded structure. The CH band was used as a standard of intensity to normalize our HOD spectra. The results are displayed in Fig. 1 which shows the integrated intensity of the OD stretch calibrated in this manner as a function of temperature. The integrated OD stretch intensity decreased by 20% as the temperature was increased from -31.5 to +160 °C. This indicates that hydrogen bonding, which occurs more readily at low temperature, enhances the Raman cross sections of the individual oscillators. The data of Fig. 1

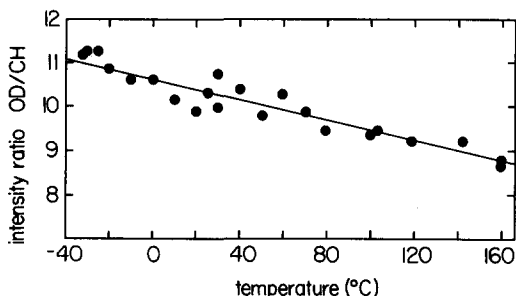


FIG. 1. Stokes Raman integrated OD stretch intensity of HOD relative to integrated CH stretch intensity of methanol (2837 cm<sup>-1</sup> band) for 1 mol % methanol in 10 mol % HOD in liquid H<sub>2</sub>O.

are adequately described by a linear relationship.

Figure 1 reflects the "correct" temperature behavior of the integrated OD stretch intensity. A second series of spectra performed to obtain  $I(\nu)$  vs  $\nu$  of the OD stretch rather than the integrated spectra were taken in water mixtures not doped with methanol. Our feeling was that if methanol affected the OD stretch it would more severely affect  $I(\nu)$  vs  $\nu$  rather than  $\int I(\nu)d\nu$ . Calibration of this second set of spectra was achieved by forcing the integrated spectra to follow the same dependency with temperature as the first, methanol doped set displayed in Fig. 1. After comparison of the doped and undoped samples, we found the effect of such a small amount of methanol could not be measured so our precautions were perhaps unwarranted. The results are the quantitative spectra of Figs. 2 and 3.

Figure 2 spans 191 °C and displays no isosbestic crossing. Figure 3 is a comparison of our results to Walrafen in the range of approximately +30 to +100 °C.<sup>2</sup> The two results are quite similar, including the apparent isosbestic behavior and its frequency. Close examination of our data shows, however, this apparent isosbestic in Fig. 3 is due to the limited range of temperatures used. In fact, the crossing of any two consecutive isotherms decreases slowly yet uniformly with temperature throughout the full range 160 to -31.5 °C. Furthermore, the lack of isosbestic behavior in Fig. 2 cannot be explained on the basis of experimental uncertainties. Hence we conclude there is not an exact isosbestic in the HOD spectrum.

#### B. Average bond energy vs frequency

We assume a one-to-one correspondence between Raman frequency shift and the energy state of the hydrogen bond of the OD oscillator. If the state multiplicity is at most a weak function of temperature, the Raman intensity should be described by the Boltzmann distribution. This would imply a graph of  $\ln[I(\nu, T)/I(\nu_0, T)]$  vs  $1/T$  should be linear with slope related to the energy difference between the states at  $\nu$  and  $\nu_0$ . Figure 4 gives three examples at different  $\nu$ . These plots are linear supporting this Boltzmann analysis. The reference frequency was chosen to be 2440 cm<sup>-1</sup> because this corresponds to the peak frequency of the frozen HOD solution near 0 °C and the peak in amorphous solid HOD. Thus the intensity at the reference frequency represents ice-like hydrogen bonded scatterers.

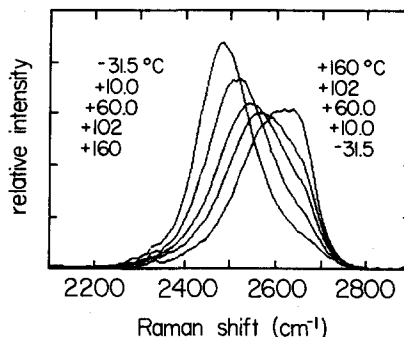


FIG. 2. Quantitative Stokes Raman isotherms for the OD stretch of 10% HOD in liquid H<sub>2</sub>O.

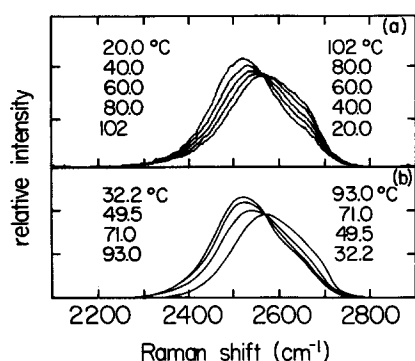


FIG. 3. A comparison of quantitative OD stretch isotherms of dilute HOD in liquid H<sub>2</sub>O in the normal liquid range. (a) This work. (b) Walrafen (Ref. 2).

The slopes of 31 plots like those in Fig. 4 are given in Fig. 5 vs  $\nu$ . Notice that there is a minimum near 2440 cm<sup>-1</sup>. This reinforces the choice of this reference frequency as the frequency of optimum, or lowest, hydrogen bond energy. For example, the scatterers at 2400 cm<sup>-1</sup> are slightly higher in energy than those at 2440 cm<sup>-1</sup> (see Fig. 4) demonstrating that lower frequency scatterers do not necessarily have stronger hydrogen bonds. Thus we find the optimum hydrogen bond in the liquid is at the same frequency as in the solid phases.

Of significance is the plateau-like region centered at 2650 cm<sup>-1</sup>. Given this region's high energy relative to the ice-like mode at 2440 cm<sup>-1</sup> and its relative independence of energy with  $\nu$ , we interpret this region to be due to hydrogen bonds that are essentially completely broken. Bansil *et al.*<sup>4</sup> also concluded that the band centered at 2650 cm<sup>-1</sup> was due to OD oscillators that were "essentially free" of hydrogen bonds. We feel this near energy independence in this plateau region is particularly significant since it indicates a class of oscillators all with the same high energy. Thus, while a distribution of hydrogen bond strengths is indicated in Fig. 5 for  $\nu < \sim 2630$  cm<sup>-1</sup>, there is at most a weak distribution of broken bond strengths, consistent with the notion that a

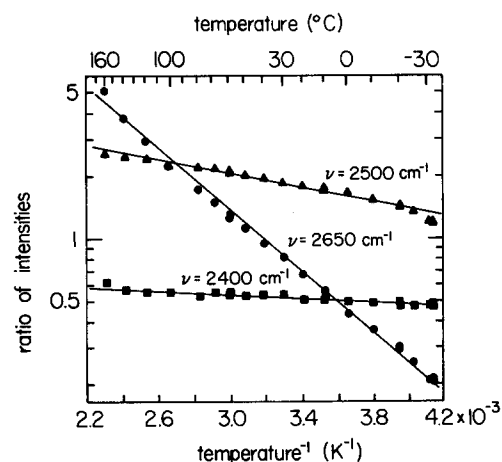


FIG. 4. Semilog plot of OD stretch intensity ratios  $I(\nu)/I(2440 \text{ cm}^{-1})$  for three different  $\nu$ 's. ■, ▲, and ● represent  $\nu = 2400, 2500$ , and  $2650 \text{ cm}^{-1}$ , respectively.

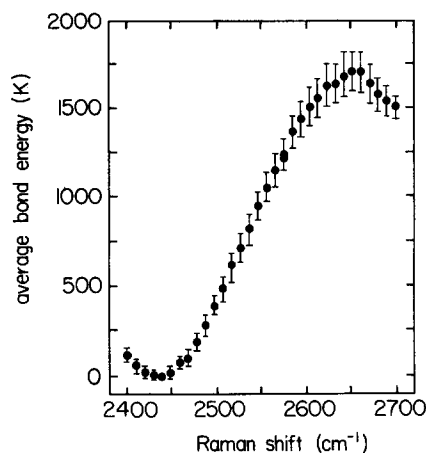


FIG. 5. Average deuterium hydrogen bond energy (in Kelvin) relative to the scatterers at 2440 cm<sup>-1</sup>. This figure is formed from the slopes of 31 plots like those in Fig. 4 (1600 K corresponds to 3.2 kcal/g mol of bonds).

bond cannot be more than broken. The energy difference relative to  $\nu_0$  is  $3.2 \pm 0.2$  kcal/g mol bonds. This would be the energy required to completely break one ice-like deuterium hydrogen bond. Earlier spectroscopy values based on two-state analysis have yielded values in the range 2.4 to 2.6 kcal/mol for hydrogen bonds.<sup>12</sup> This is an average value over the distribution of hydrogen bond strengths and should be less than our 3.2 kcal/mol which represents the strongest hydrogen bond.

### C. Two-state analysis

In spite of the absence of an exact isosbestic, a two-state analysis is still useful. The plateau region of Fig. 5 reveals remarkable uniformity in the energy of the scatterers there. That significant scattering still occurs from such high energy, relative to  $kT$ , states is not too surprising as the highly directional nature of the hydrogen bond should lead to a larger multiplicity of energetically similar nonhydrogen bonded states. This suggests that the nonhydrogen bonded (NHB) state is well approximated by a band with a fixed peak and full width at half-maximum (FWHM). Accordingly, we separated the NHB intensity out of the complete spectrum in two ways. First by reflection and hence symmetrization of the plateau intensity about its estimated center at 2650 cm<sup>-1</sup>. Second, by simple division of the spectrum into hydrogen bonded (HB) and nonhydrogen bonded (NHB)

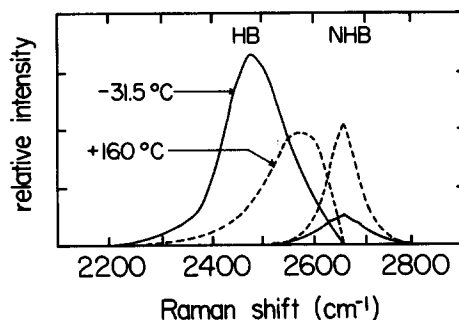


FIG. 6. Two example separations of OD stretch isotherms into NHB and HB components. The analysis assumed the intensity above 2650 cm<sup>-1</sup> to be only NHB and preformed a symmetry reflection about this frequency to estimate the remaining NHB intensity.

parts at the plateau's approximate low frequency edge at  $\nu = 2600 \text{ cm}^{-1}$ . Two of these separations for the reflection-symmetrization procedure are displayed in Fig. 6. Notice that the HB peak frequency is not stationary, but slowly increases with increasing temperature. Both Walrafen<sup>13</sup> and Scherer *et al.*<sup>3</sup> had previously reached the same conclusion using a very different separation scheme. Results for the HB and NHB peak frequencies using all three of these methods are shown in Fig. 7 where they compare well.

An iterative procedure will now yield the ratio of the NHB to HB Raman cross sections, average hydrogen bond energy, and hydrogen bond probability vs temperature. Clearly  $I_{\text{HB}}$  is proportional to hydrogen bond probability  $p$  and similarly  $I_{\text{NHB}}$  to  $(1 - p)$ . However, the proportionality constants are not the same as the HB scatterers are more efficient than their NHB counterparts. Then

$$I_{\text{NHB}}(T)/I_{\text{HB}}(T) = \chi[1 - p(T)]/p(T). \quad (1)$$

The quantity  $\chi$  may be identified as the ratio of the NHB to the HB Raman cross section. This is simply rearranged to be

$$p = I_{\text{HB}}/(I_{\text{HB}} + I_{\text{NHB}}/\chi). \quad (2)$$

This is not yet enough information to obtain  $p$  precisely because the quantity  $\chi$  is unknown. However, Fig. 1 leads to the conclusion that  $\chi < 1$  since the integrated intensity decreases with increasing temperature. In fact, it contains a quantitative relationship for the ratio of the total intensity at two different temperatures  $T_1$  and  $T_2$ ,

$$I(T_1)/I(T_2) = f(T_1, T_2). \quad (3)$$

But  $I(T) \propto p(T) + \chi[1 - p(T)]$  so that the left-hand side of the above relationship can be formulated in terms of  $\chi$ ,  $p(T_1)$ , and  $p(T_2)$ . This can be written as

$$\chi = (f_{1,2}p_2 - p_1)/[1 - p_1 - f_{1,2}(1 - p_2)], \quad (4)$$

where the subscripts refer to temperatures  $T_1$  and  $T_2$ . Now the values of  $I_{\text{HB}}$  and  $I_{\text{NHB}}$ , obtained from either deconvolution above, at two different temperatures combined with the measured value of  $f_{1,2}$  are sufficient to find  $p_1$ ,  $p_2$ , and  $\chi$ . Assume  $\chi = 1$  in Eq. (2) to approximate  $p_1$  and  $p_2$ . These values are used in Eq. (4) to obtain a better value of  $\chi$  which is fed back into Eq. (2) to improve  $p_1$  and  $p_2$ . This iterative procedure will yield these three unknowns to within 1% in

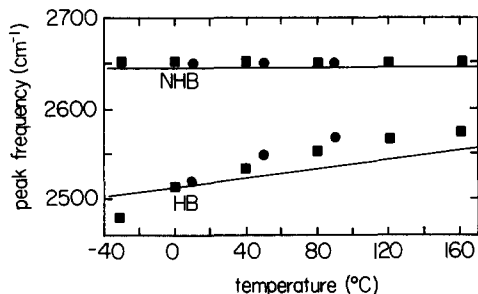


FIG. 7. Peak frequency for both the NHB and HB components resulting from three different two-state separations of the OD stretch of dilute HOD in H<sub>2</sub>O. ●, Scherer *et al.* (Ref. 3). The lines are the combined data of Lindner and Walrafen, analyzed by Walrafen (Ref. 13). ■, this work, in which the NHB peak is by definition at  $2650 \text{ cm}^{-1}$ .

about six steps. This procedure works better the larger the difference in  $T_1$  and  $T_2$ . Accordingly, for  $T_1 > 60^\circ\text{C}$ ,  $T_2 = -31.5^\circ\text{C}$  and for  $T_1 \leq 60^\circ\text{C}$ ,  $T_2 = 160^\circ\text{C}$ , the value of  $\chi$  obtained was 0.49 for the symmetrized NHB separation and 0.54 for the other method. These values are comparable to those obtained for the OH stretch in pure water by Abe and Ito,<sup>14</sup> 0.61, who compared cross sections of the liquid and the vapor, and Walrafen,<sup>15</sup> 0.59, who used isotherm difference spectra of the OH stretch in liquid H<sub>2</sub>O. The difference between our values and theirs may be due to the lack of coupling in our OD stretch data.

Figure 8 is a plot of  $\ln[(1 - p)/p]$  vs  $T^{-1}$  ( $p_{\text{HB}} = p$ ,  $p_{\text{NHB}} = 1 - p$ ). Its slope yields 1.9 kcal/g mol bonds. This is only 60% of the value obtained as the energy to completely break an ice-like deuterium hydrogen bond.

Figure 9 displays  $p$  vs  $T$ . The single bond probability is 0.8 near the singular temperature. This supports the idea that  $T_s$  is closely associated with a four bonded percolation transition. Monte Carlo simulations on an ice lattice reveal that clusters of four bonded molecules become infinite in extent at  $p = 0.795$ .<sup>5</sup>

#### D. Peak frequency and width vs $T$

Figure 10 displays the temperature dependence of the FWHM and peak frequency of the OD stretch band. The FWHM has a definite maximum around 350 K. At low temperatures the FWHM reflects the width of the HB component, whereas it reflects that of the NHB at high temperatures. The FWHM and peak frequency of the  $160^\circ\text{C}$  NHB band in Fig. 6 are  $70$  and  $2650 \text{ cm}^{-1}$ , respectively. These two values are in very good agreement with the limiting behavior of Figs. 10(a) and 10(b), respectively, hence reinforcing the consistency of our analysis. At intermediate temperatures both components have significant intensity and the width of the band is roughly the sum of the two component widths, hence the maximum. At what temperatures do these two properties extrapolate to the amorphous solid values? Peak frequency favors  $T_s = 228 \text{ K}$  over  $T_g \approx 140 \text{ K}$ . Unfortunately, the FWHM is inconclusive with regard to temperature but does support a rapid approach to the amorphous solid.

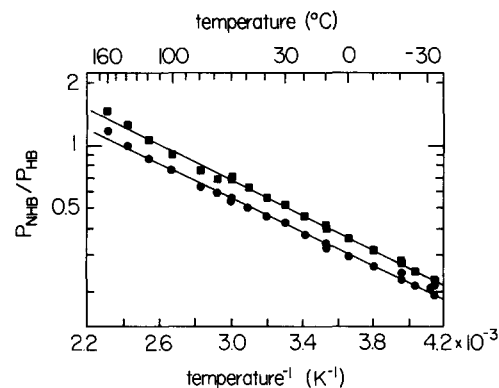


FIG. 8. Semilog plot of  $p_{\text{NHB}}/p_{\text{HB}}$  obtained from two different two-state separations of OD stretch. ■ represent all intensity above  $2600 \text{ cm}^{-1} = \text{NHB}$ , all below = HB. ● represent the NHB peak obtained by assumed symmetry and reflection about  $2650 \text{ cm}^{-1}$ .

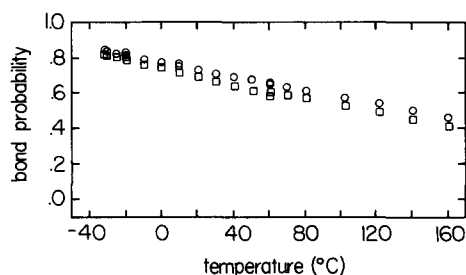


FIG. 9. Deuterium hydrogen bond probability from two different two-state separations of the OD stretch. □ represents all intensity above  $2600\text{ cm}^{-1}$  = NHB, all below = HB. ○ represent the NHB peak obtained by assumed symmetry and reflection about  $2650\text{ cm}^{-1}$ .

#### IV. DISCUSSION

Our two-state interpretation, given the data of this work, is only two state in a broad sense. Indeed, the term “two state” has been applied to many interpretations some of which have seen vigorous denunciation in the literature. Thus it is appropriate that we carefully describe what we mean by two state. As indicated by Fig. 5, the NHB oscillators display a well defined, narrow range of energies, while the HB class is quite broad. Thus, there is a clear distinction between the classes NHB and HB warranting a two-state separation, yet behavior within the HB class itself is best described by a continuum picture. This scenario has previously been described by Angell and Rodgers as the “Quasilattice with broken bonds.”<sup>16</sup> As these authors also state, this model is a true intermediate between the continuum and two-state models. This model is consistent with several aspects of the data presented here.

Angell and Rodgers who analyzed near infrared overtone spectra of H<sub>2</sub>O and HOD concluded their data were best described by a continuum model with preferential exchange of strong bonds for weak bonds. This model is only slightly less two state than the quasilattice with broken bonds model to which we would ascribe. Angell and

Rodgers remarked on how sharp the “weakly bonded” modes in their spectra were, indicating a “specific group” of such bonds similar to a broken bond class. Hence, our interpretations appear to be quite similar.

Indication of precise isosbestic points has historically supported a two-state interpretation, however, a breakdown of the isosbestic, as seen in our data, need not vitiate a quasi-two-state model. Rather, it indicates the more rigid specifications of two invariant states changing only in population must be relaxed. We find the average hydrogen bond in the HB mode gradually gets weaker with increasing temperature. This is indicated by slow increase of the peak HB frequency with increasing temperature. At the same time, there is a gross conversion of HB into NHB species. This second effect tends to dominate the first. Consequently, over a small temperature range, the peak HB frequency is approximately constant and the behavior of the spectra are approximately isosbestic as in Fig. 3. However, the gentle temperature dependence of the peak HB frequency will manifest itself over a broad temperature range as a slow increasing of the instantaneous isosbestic frequency with increasing  $T$  as seen in Fig. 2.

It is interesting to acknowledge that widely different methods of two-state separation yield the same general conclusions about the behavior of the peak frequencies of HB and NHB versus temperature. Walrafen<sup>13</sup> fitted to two Gaussian components, Scherer *et al.*<sup>3</sup> to two Gaussian-Lorentzian product functions, and symmetry of the NHB component with fixed peak frequency was used in this work. Yet these three different decompositions give the consistent results seen in Fig. 7.

Perhaps the most attractive idea underlying the two-state philosophy is the existence of a distinctive characteristic that will naturally separate all the scatterers into two classes. This distinction exists. It is evident in Fig. 5. Given this natural separation into two classes we can calculate the probability of an OH group participating in a hydrogen bond without recourse to an arbitrary definition of what is, or is not, a hydrogen bond.

In Fig. 10 the FWHM and peak frequency both display behavior that is different in the high and low temperature regimes. The high temperature data of Lindner,<sup>17</sup> which are consistent with our data in the region of mutual overlap, appear to asymptotically approach some limiting value. This indicates a slow approach to a distant, well defined NHB state with increasing temperature. In contrast, our low temperature values precipitously approach the amorphous solid values, especially the peak frequency plot, which displays no hint of asymptotic approach. With decreasing temperature, the width and peak values should principally be due to the characteristics of the HB peak which itself must be rapidly changing since asymptotic approach to the amorphous solid values is not observed. Thus we have indication of a rapid and perhaps singular approach of liquid water to a state similar to the amorphous solid as the temperature falls into the region of the singular temperature  $T_s$ .

The implication that supercooled water is approaching a state similar to the amorphous solid is not new. Angell and Rodgers saw their IR spectra lose all indication of a broken

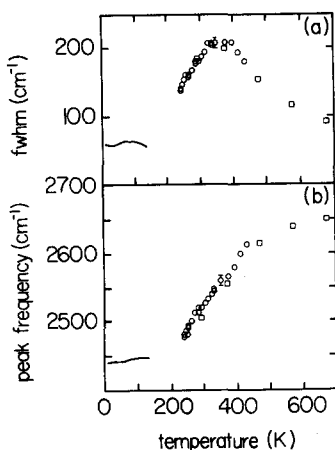


FIG. 10. (a) Full width at half-maximum and (b) peak frequency of the OD stretch of dilute HOD in liquid H<sub>2</sub>O. □ are from Lindner (Ref. 17). The solid line is for the amorphous solid from Sivakumar *et al.* (Ref. 21), and the ○ are from this work.

bond contribution as the spectra approached a form very similar to the inferred amorphous solid spectrum. Green, Lacey, and Sceats found evidence that the low frequency shoulder of the Raman OH stretch spectrum in pure H<sub>2</sub>O was developing an intensity which increased in a linear fashion to that found in ice and the amorphous solid,<sup>7</sup> becoming equal near  $T_s$ . In previous work on pure H<sub>2</sub>O we supported the Green *et al.* result and showed that the depolarization was also approaching the amorphous solid behavior.<sup>8</sup>

Of significance for this rapid approach to the amorphous solid water spectrum is the behavior of the hydrogen bond probability with declining temperature. Figure 9 indicates that the hydrogen bond probability approaches  $p_{HB} \approx 0.8$  very near the proposed singular temperature  $T_s = -45^\circ\text{C}$ . This stands in strong support of percolation theories of water which ascribe these singularities to percolation of four bonded water molecules which is predicted to occur at  $p_{HB} = 0.795$ . In earlier Raman work on pure H<sub>2</sub>O,<sup>8</sup> we presented qualitative support for  $p_{HB} \approx 0.8$  at  $T_s$ , but the coupled nature of the collective, hydrogen bonded mode incurred uncertainty in our analysis. Now, with both types of coupling absent, we again, in Fig. 9, find qualitative support of these theories. Furthermore, we reinforce our proposition from our earlier work that at  $T_s$  an infinite cluster of four bonded water molecules would form with spectral characteristics the same as those found in the amorphous solid.

The anomalous singular behavior of many thermodynamic and transport properties of supercooled water is analogous to critical point phenomena, and this has prompted theoretical interpretation using these concepts. Most notable is the work of Speedy<sup>18</sup> who has given evidence for a spinodal line in the supercooled region which represents a line of second order phase transitions relative to which various properties would appear singular. One of us has suggested analogy to binary liquid demixing critical points<sup>19,20</sup> based on the enhancement of the water anomalies upon addition of simple monohydric alcohols with hydrophobic groups which can promote water's clathrate-like structures.<sup>21,22</sup> Phase diagrams of these alcohol-water systems indicate water-water self-associating critical points in the supercooled regime.<sup>20</sup> The results of this paper cannot address the validity of these ideas. We feel that regardless of whether a critical phenomena description is appropriate, the underlying mechanism must be the rapid approach to a state similar to the amorphous solid.

What gives the NHB band its width? Eisenberg and Kauzmann<sup>23</sup> have stated that it is difficult to envision a mechanism other than variation in the hydrogen bond environment itself that could cause the large width of the stretch band, yet we claim the NHB band is not hydrogen bonded. The source of the width of the NHB band must be intramolecular coupling. The NHB OD covalent bond is only one of four hydrogen bond sites on the HOD molecule. The other three sites will have a variety of environments and hence cause a distribution of possible electronic structures for the molecule, thus causing the width of the NHB mode.

## V. CONCLUSION

We have presented Raman data for the uncoupled OD stretch band of HOD in H<sub>2</sub>O in the range  $-31.5$  to  $160^\circ\text{C}$

for liquid water. We found that an exact isosbestic did not hold for this band, instead the crossing of isotherms slowly changed with temperature. Our analysis based on Boltzmann statistics showed evidence for two types of OD oscillators: a continuum of hydrogen bonded oscillators with the frequency of the minimum energy oscillator, which correspond to the strongest hydrogen bond, nearly equal to that of either the crystalline ice or amorphous solid phase; and a band of oscillators all at  $\sim 3.2$  kcal/mol above the strongest hydrogen bond mode, which we interpreted as a broken hydrogen bond class. The lack of an exact isosbestic, which might be expected from two states, was interpreted as due to the gradual weakening of the average energy of the hydrogen bond class with temperature as evidenced by this mode's peak frequency increasing slowly with temperature. These two classes allowed us to determine a hydrogen bond probability which was seen to linearly increase with declining temperature and achieve a value of 0.8 near the singular temperature of the anomalies of supercooled water,  $T_s \approx -45^\circ\text{C}$ . This result qualitatively supports percolation theories of these anomalies which predict a four bonded percolation threshold for the water molecules at a hydrogen bond probability of 0.8. We also found that the peak frequency and full width at half-maximum of the OD stretch band showed a precipitous approach to the amorphous solid values as the temperature fell toward  $T_s$ . This rapid approach is similar to other anomalous or quasisingular behavior of various thermodynamic and transport properties in the supercooled regime, and we suggested this anomalous behavior is a result of liquid water's rapid approach to a state similar to the amorphous solid as the system percolates to form an infinite four bonded network.

## ACKNOWLEDGMENT

Acknowledgment is made to the donors of the Petroleum Research Fund, administered by the American Chemical Society for support of this research.

<sup>1</sup>T. T. Wall and D. F. Hornig, *J. Phys. Chem.* **43**, 2079 (1965).

<sup>2</sup>G. E. Walrafen, *J. Chem. Phys.* **48**, 244 (1968).

<sup>3</sup>J. R. Scherer, M. K. Go, and S. Kint, *J. Phys. Chem.* **78**, 1204 (1974).

<sup>4</sup>R. Bansil, J. Wiafe-Akenten, and J. L. Taaffe, *J. Chem. Phys.* **76**, 2221 (1982).

<sup>5</sup>A. Geiger and H. E. Stanley, *Phys. Rev. Lett.* **49**, 1985 (1982), R. L. Blumberg, H. E. Stanley, A. Geiger, and P. Mausback, *J. Chem. Phys.* **80**, 5230 (1984).

<sup>6</sup>R. J. Speedy and C. A. Angell, *J. Chem. Phys.* **65**, 851 (1976).

<sup>7</sup>J. L. Green, A. R. Lacey, and M. G. Sceats, *J. Phys. Chem.* **90**, 3958 (1986).

<sup>8</sup>D. E. Hare and C. M. Sorensen, *J. Chem. Phys.* **93**, 25 (1990).

<sup>9</sup>S. C. Mossop, *Proc. Phys. Soc. London Sect. B* **68**, 193 (1955).

<sup>10</sup>G. D'Arrigo, G. Maisano, F. Mallamace, P. Migliardo, and F. Wanderlingh, *J. Chem. Phys.* **75**, 4264 (1981).

<sup>11</sup>G. E. Walrafen, M. S. Hokmabadi, and W.-H. Yang, *J. Chem. Phys.* **85**, 6964 (1986).

<sup>12</sup>D. Eisenberg and W. Kauzmann, *The Structure and Properties of Water* (Oxford University, London, 1969), p. 101.

<sup>13</sup>G. E. Walrafen, in *Water: A Comprehensive Treatise*, edited by F. Franks (Plenum, New York, 1972), Vol. 1, Chap. 5, p. 185.

<sup>14</sup>N. Abe and M. Ito, *J. Raman Spectrosc.* **7**, 161 (1978).

<sup>15</sup>G. E. Walrafen, M. R. Fisher, M. S. Hokmabadi, and W.-H. Yang, *J. Chem. Phys.* **85**, 6970 (1986).

- <sup>16</sup>C. A. Angell and V. Rodgers, *J. Chem. Phys.* **80**, 6245 (1984).  
<sup>17</sup>H. Lindner, Doctoral dissertation, University of Karlsruhe, 1970; and in Ref. 13.  
<sup>18</sup>R. J. Speedy, *J. Phys. Chem.* **86**, 982 (1982).  
<sup>19</sup>G. W. Euliss and C. M. Sorensen, *J. Chem. Phys.* **80**, 4767 (1984).  
<sup>20</sup>C. M. Sorensen, *Int. J. Thermophys.* **9**, 703 (1988).  
<sup>21</sup>B. L. Halfpap and C. M. Sorensen, *J. Chem. Phys.* **77**, 466 (1982).  
<sup>22</sup>R. J. Speedy, J. A. Ballance, and B. D. Cornish, *J. Phys. Chem.* **87**, 325 (1983).  
<sup>23</sup>See Ref. 12, p. 239.